

Single-valley quantum Hall ferromagnet in a dilute $\text{Mg}_x\text{Zn}_{1-x}\text{O}/\text{ZnO}$ strongly correlated two-dimensional electron system

Y. Kozuka,^{1,*} A. Tsukazaki,^{1,2} D. Maryenko,³ J. Falson,^{1,†} C. Bell,^{4,5} M. Kim,^{4,5} Y. Hikita,^{4,5}
H. Y. Hwang,^{3,4,5,6} and M. Kawasaki^{1,3,6,7}

¹*Department of Applied Physics and Quantum-Phase Electronics Center (QPEC), University of Tokyo, Tokyo 113-8656, Japan*

²*PRESTO, Japan Science and Technology Agency (JST), Tokyo 102-0075, Japan*

³*Correlated Electron Research Group (CERG), RIKEN-Advanced Science Institute, Wako 351-0198, Japan*

⁴*Department of Advanced Materials Science, University of Tokyo, Kashiwa, Chiba 277-8561, Japan*

⁵*Department of Applied Physics and Stanford Institute for Materials and Energy Sciences, Stanford University, Stanford, California 94305, USA*

⁶*CREST, Japan Science and Technology Agency (JST), Tokyo 102-0075, Japan*

⁷*WPI Advanced Institute for Materials Research, Tohoku University, Sendai 980-8577, Japan*

(Received 12 January 2012; published 3 February 2012)

We investigate the spin susceptibility (g^*m^*) of dilute two-dimensional (2D) electrons confined at the $\text{Mg}_x\text{Zn}_{1-x}\text{O}/\text{ZnO}$ heterointerface. Magnetotransport measurements show a four-fold enhancement of g^*m^* , dominated by the increase in the Landé g -factor. The g -factor enhancement leads to a ferromagnetic instability of the electron gas as evidenced by sharp resistance spikes. At high magnetic field, the large g^*m^* leads to full spin polarization, where we found sudden increase in resistance around the filling factors of half-integer, accompanied by complete disappearance of fractional quantum Hall (QH) states. Along with its large effective mass and the high electron mobility, our result indicates that the ZnO 2D system is ideal for investigating the effect of electron correlations in the QH regime.

DOI: [10.1103/PhysRevB.85.075302](https://doi.org/10.1103/PhysRevB.85.075302)

PACS number(s): 73.43.Qt, 72.25.Dc, 73.40.Qv

I. INTRODUCTION

The Coulomb interaction plays a substantial role in many aspects of the transport phenomena in two-dimensional (2D) systems and can lead to the renormalization of electron characteristics such as the effective mass and the g -factor, which affects the transport and magnetic properties of the 2D carriers.¹ For instance, a 2D metallic state is experimentally observed as a consequence of electron correlations,^{2,3} although scaling theory based on non-interacting electrons predicts 2D systems to always be localized in the presence of finite disorder.⁴ The strength of the electron correlations is characterized by the Wigner-Seitz radius (r_s), which is defined as the ratio of the Coulomb energy to the Fermi energy, and expressed as $m^*e^2/4\pi\epsilon\hbar^2\sqrt{\pi n}$, where m^* is the effective mass of the charge carriers, e the elementary electric charge, ϵ the dielectric constant, \hbar Planck's constant divided by 2π , and n the charge carrier density. Accordingly, correlation effects are pronounced in diluted charge carrier systems.

So far, clean 2D systems with $r_s \gg 1$ have been studied in a number of materials such as Si-MOSFET,⁵⁻⁷ Si/SiGe,⁸ GaAs/AlGaAs,^{9,10} and AlAs/AlGaAs.¹¹⁻¹³ In these studies the enhancement of the effective spin susceptibility (g^*m^*) was universally observed, where g^* is the effective Landé g -factor. However, the dominating component driving the enhancement of this binary parameter may be linked to the valley degeneracy of the 2D charge carriers and hence is system dependent. In valley-degenerate materials, such as AlAs and Si,^{5-7,13} g^*m^* is primarily dominated by the enhancement of the effective mass, although the g -factor enhancement is also observed to some extent. This dominating parameter is interchanged when the 2D system of AlAs is driven into single valley occupancy; the g -factor enhancement prevails over the mass enhancement.¹¹⁻¹³ Similarly for GaAs, the g -factor

enhancement is stronger than the change in the electron mass.^{9,10}

Large correlation effects are also expected in the emerging field of 2D electrons confined in $\text{Mg}_x\text{Zn}_{1-x}\text{O}/\text{ZnO}$ heterostructures.¹⁴⁻¹⁶ The electrons in this novel structure occupy an isotropic single pocket as in GaAs-based 2D systems but have a larger band mass of $0.29m_0$ (m_0 is the bare electron mass). Also the smaller dielectric constant ($\epsilon = 8.5$) of ZnO strengthens the correlation effects. Thus, this system, with its high electron mobility (μ), lends itself to studies of g^*m^* enhancement in the regime of strong correlations.

Here, we investigate the magnetotransport properties of a 2D electron gas confined in a $\text{Mg}_x\text{Zn}_{1-x}\text{O}/\text{ZnO}$ heterostructure in a tilted magnetic field. The charge carrier density of our sample is $n = 2.0 \times 10^{11} \text{ cm}^{-2}$, corresponding to $r_s = 8.4$. We observe an almost four-fold enhancement of the g^*m^* with respect to its bulk value. Combined with the previous results for $\text{Mg}_x\text{Zn}_{1-x}\text{O}/\text{ZnO}$ samples with smaller r_s (Ref. 17), g^* tends to diverge as n decreases, which is indicative of a ferromagnetic instability. This result, with its simple band structure of ZnO, supports the idea that the g^* enhancement in the dilute limit is a generic consequence of electron correlations in single-valley systems. In addition, we observe sharp resistance spikes at the crossing point of two Landau levels with opposite spin orientation, which is indicative of the formation of ferromagnetic domains mediated by the enhanced g -factor. At high magnetic field, we find a dramatic increase in resistance around half-integer filling factors when the spins are fully polarized at high tilt angles. These observations, with its high μ , indicate that the ZnO 2D electron gas is a unique system suitable to investigate the effects of electron correlations on integer and fractional quantum Hall (QH) effects.

II. EXPERIMENTAL DETAILS

The $\text{Mg}_x\text{Zn}_{1-x}\text{O}/\text{ZnO}$ ($x = 0.01$) heterostructure was grown by molecular beam epitaxy utilizing distilled pure ozone as detailed in Ref. 14. Device preparation is discussed in Ref. 15. The sample was mounted on a rotation stage and measured in a dilution refrigerator equipped with a 14 T superconducting magnet. Electrical measurements were carried out using a lock-in amplifier with 10 nA excitation current at a frequency of 11 Hz. For several angles between the direction of the magnetic field and the normal to the 2D plane (θ), the four-terminal resistance was measured as a function of the magnetic field. The tilt angle θ is estimated from Hall resistance (R_{xy}) as $\cos\theta = R_{xy}(\theta)/R_{xy}(0^\circ)$ in the low field range below 0.5 T.

III. RESULTS AND DISCUSSIONS

Figure 1(a) shows magnetotransport traces of the longitudinal resistance R_{xx} as well as the Hall resistance R_{xy} of the 2D electron system at $T = 100$ mK and $\theta = 0^\circ$. A number of integer and fractional QH states are clearly observed; R_{xx} shows zero resistance while R_{xy} is quantized. From the low-field transport data, μ is estimated as $300\,000\text{ cm}^2\text{ V}^{-1}\text{ s}^{-1}$.

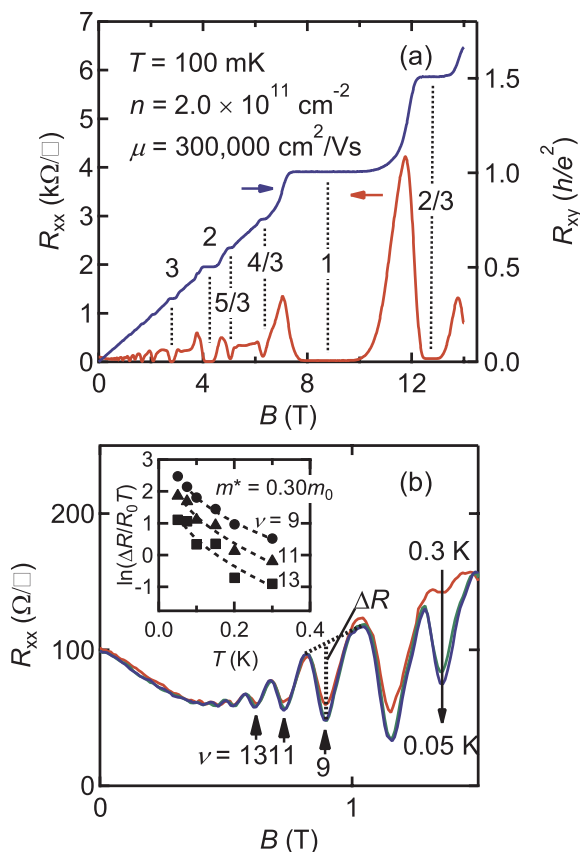


FIG. 1. (Color online) (a) R_{xx} and R_{xy} as a function of magnetic field at $T = 100$ mK. (b) Temperature dependence of the low-field Shubnikov-de Haas (SdH) oscillations from 0.05 to 0.3 K. ΔR defines the SdH amplitude. The inset shows the T dependence of $\Delta R/R_0 T$ for $\nu = 9$ (circles), 11 (triangles), and 13 (squares), where R_0 denotes R_{xx} at zero magnetic field. The dashed curves are the fits to the data for estimating m^* .

We start the discussion of the g^*m^* measurement by analyzing m^* , which is determined from the temperature dependence of the amplitude of the Shubnikov-de Haas (SdH) oscillations (ΔR) shown in Fig. 1(b). This is described by $\Delta R/R_0 = 4\chi \exp(-\pi/\omega_c\tau_q)/\sinh\chi$, where R_0 is the resistance at $B = 0$ T, $\chi = 2\pi^2 k_B T/\hbar\omega_c$ (k_B is the Boltzmann constant), $\omega_c = eB/m^*$ is the cyclotron frequency, and τ_q is the quantum scattering time.¹⁷ The inset of Fig. 1(b) depicts $\ln(\Delta R/R_0 T)$ versus T , from which the electron effective mass of $(0.30 \pm 0.02)m_0$ is determined. The quantum scattering time was also estimated as 2.2 ps from the magnetic field dependence (not shown) and was temperature independent within measurement error. The large ratio $\tau_{tr}/\tau_q = 23$ ($\tau_{tr} = \mu m^*/e$ is the transport scattering time) indicates dominant forward-scattering over back-scattering, which is typical of remote impurity scattering.¹⁸

To evaluate g^*m^* , we employ the fact that the Landau level splitting $(\hbar e/m^*)B \cos\theta$ depends on the magnetic field component normal to the 2D plane, while the Zeeman splitting $g^*\mu_B B$ (μ_B is the Bohr magneton) scales with the total magnetic field. Therefore the ratio of the Zeeman energy and the cyclotron energy can be adjusted by changing θ , so that the spin-split Landau levels cross using a geometry shown in the left inset of Fig. 2(a). The crossing of the Landau levels is experimentally found as a weakening of the SdH oscillation minima. Equating the two energy scales, the coincidence condition can be expressed as $g^*m^*/2m_0 \cos\theta_c = i$, where θ_c is the coincidence angle and i is the index difference of the crossing Landau levels. Figure 2(a) displays the magnetotransport curves for R_{xx} at several tilt angles θ as a function of the normal component of the magnetic field ($B \cos\theta$). The R_{xx} dependence on $1/\cos\theta$ is plotted in panel (b) for filling factors $\nu = 6$ and $\nu = 7$. In this plot we indicate the coincidence angles θ_c , for which the level crossings are shown by triangles.

Enforcing the linear dependence between $1/\cos\theta_c$ and the coincidence index i to go through the origin, we assign $i = 2$ and $i = 3$ to the corresponding θ_c , as shown in the inset. From the slope of the linear dependence, we estimate $g^*m^*/g_b m_b = 3.90 \pm 0.02$, where g_b and m_b are the bulk g -factor and electron mass of ZnO, respectively. In Fig. 3(a) we plot the dependence of m^*/m_b and $g^*m^*/g_b m_b$ versus charge density, together with the previously reported data by Tsukazaki *et al.* using $\text{Mg}_x\text{Zn}_{1-x}\text{O}/\text{ZnO}$ 2D electrons.¹⁹ This tendency clearly indicates that m^* moderately depends on carrier density and g^* is the dominant factor for the enhancement of g^*m^* . Since the conduction band of ZnO is composed of a single electron pocket located at the Γ point, our result of the dominance of the g^* enhancement follows the conclusion in Ref. 13, as introduced previously.

A large g -factor is a result of the enhancement of the exchange interaction J at large r_s (Refs. 20 and 21), which ultimately leads to a ferromagnetic instability. Experimentally, the formation of ferromagnetic domains is detected by sharp resistance spikes in R_{xx} as a consequence of dissipative transport across the domain wall boundaries at the crossing point of Landau levels with different spin orientations.²² Several such spikes are visible in Fig. 2(a) at tilt angles corresponding to the coincidence condition. The resistance spikes appear beyond $B \cos\theta \sim 1.5$ T ($\nu < 5$), which suggests that the condition for Stoner ferromagnetism is

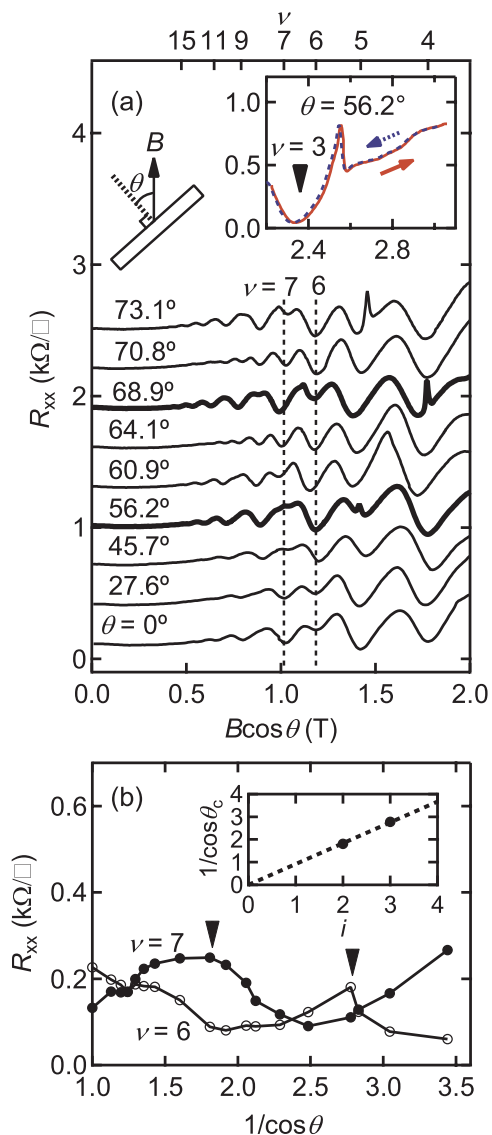


FIG. 2. (Color online) (a) R_{xx} as a function of $B \cos \theta$ at various θ . The curves are shifted upward for clarity. The top axis shows the corresponding ν . The left inset shows the geometry of the measurement. The right inset shows R_{xx} near the resistance spike at $\theta = 56.2^\circ$ near $\nu = 3$ with increasing (solid curve) and decreasing (dashed curve) magnetic field. (b) R_{xx} as a function of $1/\cos \theta$ for $\nu = 6$ (open circles) and $\nu = 7$ (filled circles). The inset shows $1/\cos \theta_c$ as a function of coincidence factor (i), where θ_c is the coincidence angle. The dashed line indicates a linear fit to the data.

fulfilled in this range.²³ Such resistance spikes have also been experimentally observed in other 2D systems^{24–29} and were commonly accompanied with hysteresis.²⁶ However, in our measurement, hysteresis is absent, as shown in the right inset of Fig. 2(a). This observation may imply that the domain walls move easily, as expected for clean ferromagnets.²⁷

It is important to note that the longitudinal resistance R_{xx} is enhanced significantly with increasing tilt angle θ at lower half-integer filling factors. Figure 4(a) shows that R_{xx} increases around $\nu = 3/2, 5/2,$ and $7/2$ with increasing θ and is accompanied with the disappearance of the fractional QH states in the first Landau level. In order to investigate the origin

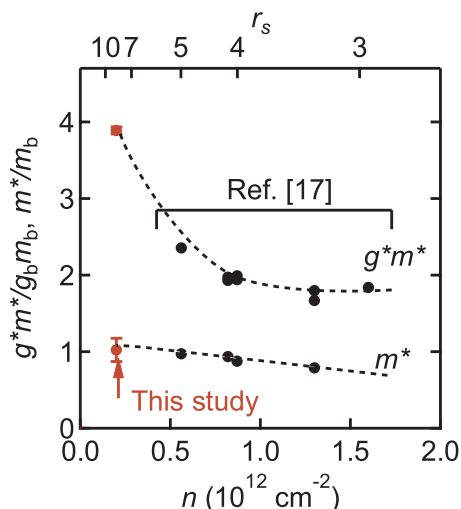


FIG. 3. (Color online) g^*m^* and m^* with respect to bulk values as a function of n together with the data from the previous report (Ref. 17). Top axis shows the corresponding r_s .

of the resistance increase, we plot R_{xx} at these filling factors as a function of θ in Fig. 4(b) and as a function of the total magnetic field B in Fig. 4(c). This comparison clearly shows that R_{xx} increases at the same B for all three half-integer filling factors and saturates at almost the same R_{xx} value. Such scaling with total magnetic field is indicative of a spin effect rather than as a result of electron orbital motion. In this

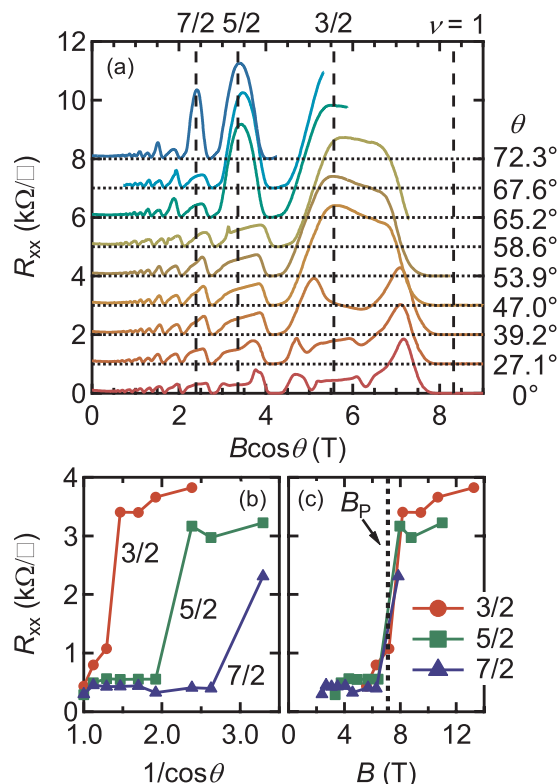


FIG. 4. (Color online) (a) R_{xx} as a function of $B \cos \theta$ for a variety of θ . R_{xx} at $\nu = 3/2, 5/2,$ and $7/2$ as a function of (b) $1/\cos \theta$ and (c) B . The dashed line in (c) indicates the critical magnetic field above which spins are fully polarized (B_p).

context it is instructive to estimate the magnetic field strength B_p at which the spins are fully polarized, which results in $B_p = (2h/e)n/g^*m^* = 7.0$ T for our sample. As Fig. 4(c) shows, this value of B_p agrees well with the experimental observation of the sharp resistance increase and thus supports its spin related origin. A similar spin-dependent increase in R_{xx} at half-filling factors has been observed only in AlAs quantum wells with single-valley occupancy.³⁰ The model to explain such a behavior takes into account a reduction in inter-Landau level screening between channels with opposite spins and thus an increased scattering rate, i.e., increased resistance. We note for our system that the fractional QH effect at $\nu > 1$ completely disappears in the ferromagnetic state. This result sheds renewed light on the problem of the stability of the fractional QH effect at the second Landau level, which has been intensively studied in the GaAs 2D electron gas.³¹

IV. CONCLUSIONS

We have investigated g^*m^* of a dilute electron gas confined at a $\text{Mg}_x\text{Zn}_{1-x}\text{O}/\text{ZnO}$ heterointerface as a prototype correlated 2D system with single-valley occupation. The result showed that spin susceptibility is enhanced with the dominant contribution from the g -factor rather than the effective mass, which is indicative of a ferromagnetic instability as

a result of enhanced exchange interactions. Experimental confirmation of the existence of ferromagnetic domains was achieved using the sharp resistance spikes at the coincidence angle. Additionally, an increase in the magnetoresistance was observed around half-integer filling factors when the spins are fully polarized. Along with the extremely high μ of the 2D electrons and the isotropic single electron pocket, these facts demonstrate that the $\text{Mg}_x\text{Zn}_{1-x}\text{O}/\text{ZnO}$ heterostructure is a suitable system to investigate the relationship between spin polarization and the integer and fractional QH effects.

ACKNOWLEDGMENTS

This work was partly supported by Grant-in-Aids for Scientific Research No. 22840004 (Y.K.) from MEXT, Japan, and by ‘‘Funding Program for World-Leading Innovative R&D on Science and Technology (FIRST)’’ Program from the Japan Society for the Promotion of Science (JSPS) initiated by the Council for Science and Technology Policy (A.T.) as well as by Asahi Glass Foundation (Y.K. and M.K.). C.B., M.K., Y.H., and H.Y.H. acknowledge support by the Department of Energy, Office of Basic Energy Sciences, Division of Materials Sciences and Engineering, under contract DE-AC02-76SF00515.

*kozuka@ap.t.u-tokyo.ac.jp

[†]On leave from the Institute for Materials Research, Tohoku University.

¹A. A. Shashkin, *Phys. Usp.* **48**, 129 (2005).

²S. V. Kravchenko, G. V. Kravchenko, J. E. Furneaux, V. M. Pudalov, and M. D’Iorio, *Phys. Rev. B* **50**, 8039 (1994).

³A. Punnoose and A. M. Finkel’stein, *Science* **310**, 289 (2005).

⁴E. Abrahams, P. W. Anderson, D. C. Licciardello, and T. V. Ramakrishnan, *Phys. Rev. Lett.* **42**, 673 (1979).

⁵A. A. Shashkin, S. V. Kravchenko, V. T. Dolgoplov, and T. M. Klapwijk, *Phys. Rev. Lett.* **87**, 086801 (2001).

⁶A. A. Shashkin, S. V. Kravchenko, V. T. Dolgoplov, and T. M. Klapwijk, *Phys. Rev. B* **66**, 073303 (2002).

⁷A. A. Shashkin, M. Rahimi, S. Anissimova, S. V. Kravchenko, V. T. Dolgoplov, and T. M. Klapwijk, *Phys. Rev. Lett.* **91**, 046403 (2003).

⁸K. Lai, T. M. Lu, W. Pan, D. C. Tsui, S. Lyon, J. Liu, Y. H. Xie, M. Mühlberger, and F. Schäffler, *Phys. Rev. B* **73**, 161301(R) (2006).

⁹J. Zhu, H. L. Stormer, L. N. Pfeiffer, K. W. Baldwin, and K. W. West, *Phys. Rev. Lett.* **90**, 056805 (2003).

¹⁰Y.-W. Tan, J. Zhu, H. L. Stormer, L. N. Pfeiffer, K. W. Baldwin, and K. W. West, *Phys. Rev. Lett.* **94**, 016405 (2005).

¹¹K. Vakili, Y. P. Shkolnikov, E. Tutuc, E. P. De Poortere, and M. Shayegan, *Phys. Rev. Lett.* **92**, 226401 (2004).

¹²T. Gokmen, M. Padmanabhan, E. Tutuc, M. Shayegan, S. De Palo, S. Moroni, and G. Senatore, *Phys. Rev. B* **76**, 233301 (2007).

¹³T. Gokmen, M. Padmanabhan, and M. Shayegan, *Phys. Rev. B* **81**, 235305 (2010).

¹⁴J. Falson, D. Maryenko, Y. Kozuka, A. Tsukazaki, and M. Kawasaki, *Appl. Phys. Express* **4**, 091101 (2011).

¹⁵A. Tsukazaki, S. Akasaka, K. Nakahara, Y. Ohno, H. Ohno, D. Maryenko, A. Ohtomo, and M. Kawasaki, *Nat. Mater.* **9**, 889 (2010).

¹⁶Y. Kozuka, A. Tsukazaki, D. Maryenko, J. Falson, S. Akasaka, K. Nakahara, S. Nakamura, S. Awaji, K. Ueno, and M. Kawasaki, *Phys. Rev. B* **84**, 033304 (2011).

¹⁷L. Smrčka, H. Havlova, and A. Isihara, *J. Phys. C* **19**, L475 (1986).

¹⁸U. Bockelmann, G. Abstreiter, G. Weimann, and W. Schlapp, *Phys. Rev. B* **41**, 7864 (1990).

¹⁹A. Tsukazaki, A. Ohtomo, M. Kawasaki, S. Akasaka, H. Yuji, K. Tamura, K. Nakahara, T. Tanabe, A. Kamisawa, T. Gokmen, J. Shabani, and M. Shayegan, *Phys. Rev. B* **78**, 233308 (2008).

²⁰J. F. Janak, *Phys. Rev.* **178**, 1416 (1969).

²¹B. Tanatar and D. M. Ceperley, *Phys. Rev. B* **39**, 5005 (1989).

²²T. Jungwirth and A. H. MacDonald, *Phys. Rev. Lett.* **87**, 216801 (2001).

²³B. A. Piot, D. K. Maude, M. Henini, Z. R. Wasilewski, K. J. Friedland, R. Hey, K. H. Ploog, A. I. Toropov, R. Airey, and G. Hill, *Phys. Rev. B* **72**, 245325 (2005).

²⁴J. Jaroszyński, T. Andrearczyk, G. Karczewski, J. Wróbel, T. Wojtowicz, E. Papis, E. Kamińska, A. Piotrowska, D. Popović, and T. Dietl, *Phys. Rev. Lett.* **89**, 266802 (2002).

²⁵E. P. De Poortere, E. Tutuc, S. J. Papadakis, and M. Shayegan, *Science* **290**, 1546 (2000).

²⁶E. P. De Poortere, E. Tutuc, and M. Shayegan, *Phys. Rev. Lett.* **91**, 216802 (2003).

²⁷K. Muraki, T. Saku, and Y. Hirayama, *Phys. Rev. Lett.* **87**, 196801 (2001).

- ²⁸J. C. Chokomakoua, N. Goel, S. J. Chung, M. B. Santos, J. L. Hicks, M. B. Johnson, and S. Q. Murphy, *Phys. Rev. B* **69**, 235315 (2004).
- ²⁹K. Toyama, T. Nishioka, K. Sawano, Y. Shiraki, and T. Okamoto, *Phys. Rev. Lett.* **101**, 016805 (2008).

- ³⁰K. Vakili, Y. P. Shkolnikov, E. Tutuc, N. C. Bishop, E. P. De Poortere, and M. Shayegan, *Phys. Rev. Lett.* **94**, 176402 (2005).
- ³¹V. W. Scarola, K. Park, and J. K. Jain, *Phys. Rev. B* **62**, 16259(R) (2000).